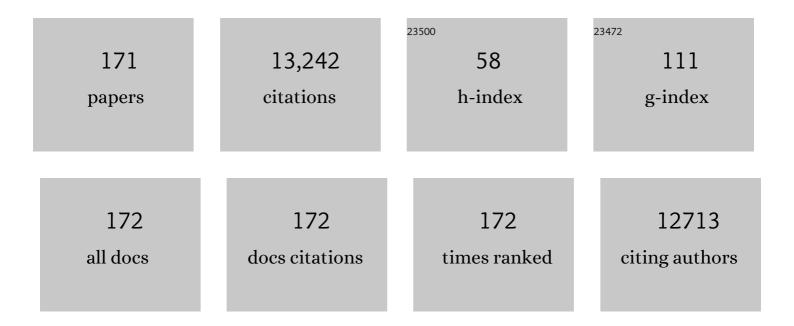
List of Publications by Year in descending order

Source: https://exaly.com/author-pdf/6909124/publications.pdf Version: 2024-02-01



LEE | DICHTED

#	Article	IF	CITATIONS
1	CO <sub>2</sub> electrolysis to multicarbon products at activities greater than 1 A cm <sup>â^2</sup> . Science, 2020, 367, 661-666.	6.0	860
2	Optical properties of coupled metallic nanorods for field-enhanced spectroscopy. Physical Review B, 2005, 71, .	1.1	534
3	Molecular origin of high field-effect mobility in an indacenodithiophene–benzothiadiazole copolymer. Nature Communications, 2013, 4, 2238.	5.8	456
4	Contact-induced crystallinity for high-performance soluble acene-based transistors and circuits. Nature Materials, 2008, 7, 216-221.	13.3	455
5	Semiconducting Thienothiophene Copolymers: Design, Synthesis, Morphology, and Performance in Thinâ€Film Organic Transistors. Advanced Materials, 2009, 21, 1091-1109.	11.1	412
6	Molecular Packing of High-Mobility Diketo Pyrrolo-Pyrrole Polymer Semiconductors with Branched Alkyl Side Chains. Journal of the American Chemical Society, 2011, 133, 15073-15084.	6.6	381
7	Efficient electrically powered CO2-to-ethanol via suppression of deoxygenation. Nature Energy, 2020, 5, 478-486.	19.8	363
8	Vibrationally resolved sum-frequency generation with broad-bandwidth infrared pulses. Optics Letters, 1998, 23, 1594.	1.7	335
9	Critical Role of Side-Chain Attachment Density on the Order and Device Performance of Polythiophenes. Macromolecules, 2007, 40, 7960-7965.	2.2	321
10	Anisotropic Structure and Charge Transport in Highly Strainâ€Aligned Regioregular Poly(3â€hexylthiophene). Advanced Functional Materials, 2011, 21, 3697-3705.	7.8	288
11	Laser-excited hot-electron induced desorption: A theoretical model applied to NO/Pt(111). Surface Science, 1990, 235, 317-333.	0.8	283
12	High Carrier Mobility Polythiophene Thin Films: Structure Determination by Experiment and Theory. Advanced Materials, 2007, 19, 833-837.	11.1	276
13	Molecular Order in High-Efficiency Polymer/Fullerene Bulk Heterojunction Solar Cells. ACS Nano, 2011, 5, 8248-8257.	7.3	260
14	Variations in Semiconducting Polymer Microstructure and Hole Mobility with Spin-Coating Speed. Chemistry of Materials, 2005, 17, 5610-5612.	3.2	217
15	Measuring Molecular Order in Poly(3-alkylthiophene) Thin Films with Polarizing Spectroscopies. Langmuir, 2007, 23, 834-842.	1.6	216
16	Molecular Characterization of Organic Electronic Films. Advanced Materials, 2011, 23, 319-337.	11.1	215
17	Correlations between Mechanical and Electrical Properties of Polythiophenes. ACS Nano, 2010, 4, 7538-7544.	7.3	210
18	Stateâ€resolved evidence for hot carrier driven surface reactions: Laserâ€induced desorption of NO from Pt(111). Journal of Chemical Physics, 1989, 91, 6429-6446.	1.2	205

#	Article	IF	CITATIONS
19	Substrate-dependent interface composition and charge transport in films for organic photovoltaics. Applied Physics Letters, 2009, 94, .	1.5	196
20	Interfacial Segregation in Polymer/Fullerene Blend Films for Photovoltaic Devices. Macromolecules, 2010, 43, 3828-3836.	2.2	182
21	Absolute Molecular Orientational Distribution of the Polystyrene Surface. Journal of Physical Chemistry B, 2001, 105, 2785-2791.	1.2	180
22	Optically Driven Surface Reactions: Evidence for the Role of Hot Electrons. Physical Review Letters, 1988, 61, 1321-1324.	2.9	172
23	Morphology changes upon scaling a high-efficiency, solution-processed solar cell. Energy and Environmental Science, 2016, 9, 2835-2846.	15.6	170
24	Controlling the Orientation of Terraced Nanoscale "Ribbons―of a Poly(thiophene) Semiconductor. ACS Nano, 2009, 3, 780-787.	7.3	160
25	Morphology Development in Solution-Processed Functional Organic Blend Films: An In Situ Viewpoint. Chemical Reviews, 2017, 117, 6332-6366.	23.0	145
26	In Situ Back ontact Passivation Improves Photovoltage and Fill Factor in Perovskite Solar Cells. Advanced Materials, 2019, 31, e1807435.	11.1	143
27	Sub-picosecond charge-transfer at near-zero driving force in polymer:non-fullerene acceptor blends and bilayers. Nature Communications, 2020, 11, 833.	5.8	130
28	Correlating Stiffness, Ductility, and Morphology of Polymer:Fullerene Films for Solar Cell Applications. Advanced Energy Materials, 2013, 3, 399-406.	10.2	127
29	Efficient upgrading of CO to C3 fuel using asymmetric C-C coupling active sites. Nature Communications, 2019, 10, 5186.	5.8	127
30	Use of Xâ€Ray Diffraction, Molecular Simulations, and Spectroscopy to Determine the Molecular Packing in a Polymerâ€Fullerene Bimolecular Crystal. Advanced Materials, 2012, 24, 6071-6079.	11.1	126
31	In Situ Characterization of Polymer–Fullerene Bilayer Stability. Macromolecules, 2015, 48, 383-392.	2.2	126
32	3D Nanoscale Characterization of Thin-Film Organic Photovoltaic Device Structures via Spectroscopic Contrast in the TEM 1. Journal of Physical Chemistry C, 2010, 114, 17501-17508.	1.5	115
33	Molecular Basis of Mesophase Ordering in a Thiophene-Based Copolymer. Macromolecules, 2008, 41, 5709-5715.	2.2	114
34	Alkanethiols on Platinum: Multicomponent Self-Assembled Monolayers. Langmuir, 2006, 22, 2578-2587.	1.6	113
35	Dynamical evolution of the 2D/3D interface: a hidden driver behind perovskite solar cell instability. Journal of Materials Chemistry A, 2020, 8, 2343-2348.	5.2	112
36	Immobilization of streptavidin on 4H–SiC for biosensor development. Applied Surface Science, 2012, 258, 6056-6063.	3.1	107

#	Article	IF	CITATIONS
37	Vertically Segregated Structure and Properties of Small Molecule–Polymer Blend Semiconductors for Organic Thinâ€Film Transistors. Advanced Functional Materials, 2013, 23, 366-376.	7.8	106
38	Template Fabrication of Protein-Functionalized Goldâ^'Polypyrroleâ^'Gold Segmented Nanowires. Chemistry of Materials, 2004, 16, 3431-3438.	3.2	104
39	In Situ Morphology Studies of the Mechanism for Solution Additive Effects on the Formation of Bulk Heterojunction Films. Advanced Energy Materials, 2015, 5, 1400975.	10.2	102
40	Femtosecond Laser-Induced Desorption of CO from Cu(100): Comparison of Theory and Experiment. Physical Review Letters, 1996, 77, 4576-4579.	2.9	98
41	Effect of Processing Additives on the Solidification of Bladeâ€Coated Polymer/Fullerene Blend Films via Inâ€Situ Structure Measurements. Advanced Energy Materials, 2013, 3, 938-948.	10.2	96
42	A simple and robust approach to reducing contact resistance in organic transistors. Nature Communications, 2018, 9, 5130.	5.8	96
43	Effect of Solution Shearing Method on Packing and Disorder of Organic Semiconductor Polymers. Chemistry of Materials, 2015, 27, 2350-2359.	3.2	92
44	Comparison of Siâ^'Oâ^'C Interfacial Bonding of Alcohols and Aldehydes on Si(111) Formed from Dilute Solution with Ultraviolet Irradiation. Langmuir, 2005, 21, 882-889.	1.6	81
45	The populations of bridge and top site CO on Rh(100) vs coverage, temperature, and during reaction with O. Journal of Chemical Physics, 1987, 87, 6710-6721.	1.2	78
46	Morphological Origin of Charge Transport Anisotropy in Aligned Polythiophene Thin Films. Advanced Functional Materials, 2014, 24, 3422-3431.	7.8	77
47	Advanced Ellipsometric Characterization of Conjugated Polymer Films. Advanced Functional Materials, 2014, 24, 2116-2134.	7.8	76
48	Dielectric Response of Aligned Semiconducting Single-Wall Nanotubes. Physical Review Letters, 2007, 98, 147402.	2.9	74
49	In Situ Ellipsometric Study of PEGâ^•Cl[sup â^'] Coadsorption on Cu, Ag, and Au. Journal of the Electrochemical Society, 2005, 152, C403.	1.3	73
50	Positionâ€sensitive detector performance and relevance to timeâ€resolved electron energy loss spectroscopy. Review of Scientific Instruments, 1986, 57, 1469-1482.	0.6	67
51	The influence of adsorbate–adsorbate interactions on surface structure: The coadsorption of CO and H2 on Rh(100). Journal of Chemical Physics, 1987, 86, 477-490.	1.2	67
52	Controlling the Microstructure of Solution-Processable Small Molecules in Thin-Film Transistors through Substrate Chemistry. Chemistry of Materials, 2011, 23, 1194-1203.	3.2	67
53	Vibrational spectroscopy of H on Pt(111): Evidence for universally soft parallel modes. Physical Review B, 1987, 36, 9797-9800.	1.1	66
54	Mechanistic studies of photoinduced reactions at semiconductor surfaces. Progress in Surface Science, 1992, 39, 155-226.	3.8	65

LEE J RICHTER

#	Article	IF	CITATIONS
55	Blade Coating Aligned, High-Performance, Semiconducting-Polymer Transistors. Chemistry of Materials, 2018, 30, 1924-1936.	3.2	63
56	Optical Characterization of Oligo(phenyleneâ^'ethynylene) Self-Assembled Monolayers on Gold. Journal of Physical Chemistry B, 2004, 108, 12547-12559.	1.2	62
57	Poly(sulfobetaine methacrylate)s as Electrode Modifiers for Inverted Organic Electronics. Journal of the American Chemical Society, 2015, 137, 540-549.	6.6	62
58	Selective study of polymer/dielectric interfaces with vibrationally resonant sum frequency generation via thin-film interference. Applied Physics Letters, 2002, 80, 3084-3086.	1.5	60
59	Correlation of molecular orientation with adhesion at polystyrene/solid interfaces. Chemical Physics Letters, 2002, 363, 161-168.	1.2	60
60	A Chemically Orthogonal Hole Transport Layer for Efficient Colloidal Quantum Dot Solar Cells. Advanced Materials, 2020, 32, e1906199.	11.1	59
61	Origin of Nanoscale Variations in Photoresponse of an Organic Solar Cell. Nano Letters, 2010, 10, 1611-1617.	4.5	58
62	Competitive Adsorption of PEG, Cl[sup â^'], and SPS/MPS on Cu: An In Situ Ellipsometric Study. Journal of the Electrochemical Society, 2006, 153, C557.	1.3	55
63	High performance airbrushed organic thin film transistors. Applied Physics Letters, 2010, 96, .	1.5	55
64	Electrical and Spectroscopic Characterization of Metal/Monolayer/Si Devices. Journal of Physical Chemistry B, 2005, 109, 21836-21841.	1.2	54
65	Kinetics of unimolecular decomposition on surfaces: Methanol on Ni(110). Journal of Chemical Physics, 1985, 83, 2569-2582.	1.2	52
66	Potential Dependence of Competitive Adsorption of PEG, Cl[sup â^'], and SPS/MPS on Cu. Journal of the Electrochemical Society, 2007, 154, D277.	1.3	51
67	Formation of Silicon-Based Molecular Electronic Structures Using Flip-Chip Lamination. Journal of the American Chemical Society, 2009, 131, 12451-12457.	6.6	48
68	SEIRAS Study of Chloride-Mediated Polyether Adsorption on Cu. Journal of Physical Chemistry C, 2018, 122, 21933-21951.	1.5	48
69	Nonâ€Boltzmann rotational and inverted spin–orbit state distributions for laserâ€induced desorption of NO from Pt(111). Journal of Chemical Physics, 1988, 89, 5344-5345.	1.2	47
70	Depletion-electric-field-induced second-harmonic generation near oxidized GaAs(001) surfaces. Physical Review B, 1997, 55, 10694-10706.	1.1	47
71	Volume Expansion Caused by Water Penetration into Silica Glass. Journal of the American Ceramic Society, 2015, 98, 78-87.	1.9	47
72	Crystal Orientation Drives the Interface Physics at Two/Three-Dimensional Hybrid Perovskites. Journal of Physical Chemistry Letters, 2019, 10, 5713-5720.	2.1	47

#	Article	IF	CITATIONS
73	In Situ, Vibrationally Resonant Sum Frequency Spectroscopy Study of the Self-Assembly of Dioctadecyl Disulfide on Gold. Langmuir, 2002, 18, 7549-7556.	1.6	46
74	Stateâ€resolved studies of the laserâ€induced desorption of NO from Si(111) 7×7: Low coverage results. Journal of Chemical Physics, 1992, 96, 2324-2338.	1.2	45
75	Direct Correlation of Charge Transfer Absorption with Molecular Donor:Acceptor Interfacial Area via Photothermal Deflection Spectroscopy. Journal of the American Chemical Society, 2015, 137, 5256-5259.	6.6	45
76	Higher order effects in organic LEDs with sub-bandgap turn-on. Nature Communications, 2019, 10, 227.	5.8	45
77	Thin Film Microstructure of a Solution Processable Pyrene-Based Organic Semiconductor. Chemistry of Materials, 2008, 20, 5743-5749.	3.2	44
78	Observation of significant nitrogen–oxygen bond weakening in nitric oxide on Rh(100). Journal of Vacuum Science and Technology A: Vacuum, Surfaces and Films, 1986, 4, 1487-1490.	0.9	43
79	Multidetector electron energyâ€loss spectrometer for timeâ€resolved surface studies. Review of Scientific Instruments, 1988, 59, 22-44.	0.6	43
80	Scanning near-field infrared microscopy and spectroscopy with a broadband laser source. Journal of Applied Physics, 2000, 88, 4832.	1.1	43
81	Characterization and Control of Lipid Layer Fluidity in Hybrid Bilayer Membranes. Journal of the American Chemical Society, 2007, 129, 2094-2100.	6.6	42
82	Influence of substrate on crystallization in polythiophene/fullerene blends. Solar Energy Materials and Solar Cells, 2011, 95, 1375-1381.	3.0	42
83	Real-time X-ray scattering studies of film evolution in high performing small-molecule–fullerene organic solar cells. Journal of Materials Chemistry A, 2015, 3, 8764-8771.	5.2	42
84	Structure of Polystyrene at the Interface with Various Liquids. Macromolecules, 2004, 37, 7742-7746.	2.2	40
85	<i>In Situ</i> Observation of Alignment Templating by Seed Crystals in Highly Anisotropic Polymer Transistors. Chemistry of Materials, 2019, 31, 4133-4147.	3.2	40
86	Surface-state-mediated photochemistry: Laser-induced desorption of NO from Si(111). Physical Review Letters, 1990, 65, 1957-1960.	2.9	38
87	Reactive adsorption of H2CO on Ni(110) at 95 K. Journal of Chemical Physics, 1985, 83, 2165-2169.	1.2	37
88	Coadsorption-induced site changes: Bridging hydrogen from CO and H on Rh(100). Surface Science, 1988, 195, L182-L192.	0.8	37
89	Structural and Chemical Characterization of Monofluoro-Substituted Oligo(phenyleneâ^'ethynylene) Thiolate Self-Assembled Monolayers on Gold. Langmuir, 2004, 20, 6195-6205.	1.6	37
90	Temperature progammed electron energy loss spectroscopy: Kinetics of CH3 OH decomposition on Ni(110). Chemical Physics Letters, 1984, 111, 185-189.	1.2	36

#	Article	IF	CITATIONS
91	Electron-energy-loss spectroscopy of H adsorbed on Rh(100): Interpretation of overtone spectra as two-phonon bound states. Physical Review B, 1988, 38, 10403-10420.	1.1	36
92	Film morphology evolution during solvent vapor annealing of highly efficient small molecule donor/acceptor blends. Journal of Materials Chemistry A, 2016, 4, 15511-15521.	5.2	35
93	Origin of Differing Reactivities of Aliphatic Chains on Hâ^'Si(111) and Oxide Surfaces with Metal. Journal of Physical Chemistry C, 2007, 111, 9384-9392.	1.5	34
94	CO adsorption site occupations on Fe(111) vs coverage and temperature: The kinetics of adsorption and reaction. Journal of Chemical Physics, 1989, 90, 2050-2062.	1.2	33
95	Constraints on the use of polarization and angle-of-incidence to characterize surface photoreactions. Chemical Physics Letters, 1991, 186, 423-426.	1.2	33
96	A Low‣welling Polymeric Mixed Conductor Operating in Aqueous Electrolytes. Advanced Materials, 2021, 33, e2005723.	11.1	33
97	Control Over Ligand Exchange Reactivity in Hole Transport Layer Enables High-Efficiency Colloidal Quantum Dot Solar Cells. ACS Energy Letters, 2021, 6, 468-476.	8.8	32
98	Summary Abstract: Vibrational modes of hydrogen adsorbed on Rh(100) and their relevance to desorption kinetics. Journal of Vacuum Science and Technology A: Vacuum, Surfaces and Films, 1987, 5, 453-454.	0.9	31
99	Stable Postfullerene Solar Cells via Direct C–H Arylation Polymerization. Morphology–Performance Relationships. Chemistry of Materials, 2019, 31, 4313-4321.	3.2	31
100	Demonstration of Molecular Assembly on Si (100) for CMOS-Compatible Molecule-Based Electronic Devices. Journal of the American Chemical Society, 2008, 130, 4259-4261.	6.6	29
101	Realâ€Time Photoluminescence Studies of Structure Evolution in Organic Solar Cells. Advanced Energy Materials, 2016, 6, 1502011.	10.2	29
102	Probing Charge Recombination Dynamics in Organic Photovoltaic Devices under Open ircuit Conditions. Advanced Energy Materials, 2014, 4, 1400356.	10.2	28
103	Morphological characterization of fullerene and fullerene-free organic photovoltaics by combined real and reciprocal space techniques. Journal of Materials Research, 2017, 32, 1921-1934.	1.2	28
104	Versatile temperature controller for the investigation of surface phenomena. Review of Scientific Instruments, 1984, 55, 732-736.	0.6	27
105	Determination of Lipid Phase Transition Temperatures in Hybrid Bilayer Membranes. Langmuir, 2006, 22, 8333-8336.	1.6	25
106	Scatterometry for in situ measurement of pattern reflow in nanoimprinted polymers. Applied Physics Letters, 2008, 93, 233105.	1.5	25
107	Side chain engineering control of mixed conduction in oligoethylene glycol-substituted polythiophenes. Journal of Materials Chemistry A, 2021, 9, 21410-21423.	5.2	25
108	Molecular devices formed by direct monolayer attachment to silicon. Solid-State Electronics, 2004, 48, 1747-1752.	0.8	24

#	Article	IF	CITATIONS
109	Classification of semiconducting polymeric mesophases to optimize device postprocessing. Journal of Polymer Science, Part B: Polymer Physics, 2015, 53, 1641-1653.	2.4	23
110	In Situ X-ray Scattering Studies of the Influence of an Additive on the Formation of a Low-Bandgap Bulk Heterojunction. Chemistry of Materials, 2017, 29, 2283-2293.	3.2	23
111	The deuterium kinetic isotope effect in the decomposition of methanol on Ni(110). Journal of Vacuum Science and Technology A: Vacuum, Surfaces and Films, 1985, 3, 1549-1553.	0.9	22
112	Improved multidetector for timeâ€resolved electron energy loss spectroscopy. Review of Scientific Instruments, 1989, 60, 12-16.	0.6	22
113	An In Situ Ellipsometric Study of Cl[sup â^']-Induced Adsorption of PEG on Ru and on Underpotential Deposited Cu on Ru. Journal of the Electrochemical Society, 2006, 153, C235.	1.3	22
114	Simple transfer from spin coating to blade coating through processing aggregated solutions. Journal of Materials Chemistry A, 2017, 5, 20687-20695.	5.2	21
115	Removing optical artifacts in near-field scanning optical microscopy by using a three-dimensional scanning mode. Journal of Applied Physics, 1999, 86, 2785-2789.	1.1	20
116	Dithiol-based modification of poly(dopamine): enabling protein resistance via short-chain ethylene oxide oligomers. Chemical Communications, 2015, 51, 6591-6594.	2.2	19
117	Confinement and Processing Can Alter the Morphology and Periodicity of Bottlebrush Block Copolymers in Thin Films. ACS Nano, 2020, 14, 17476-17486.	7.3	19
118	Modeling illumination-mode near-field optical microscopy of Au nanoparticles. Journal of the Optical Society of America A: Optics and Image Science, and Vision, 2001, 18, 704.	0.8	18
119	Impact of varying side chain structure on organic electrochemical transistor performance: a series of oligoethylene glycol-substituted polythiophenes. Journal of Materials Chemistry A, 2022, 10, 10738-10749.	5.2	18
120	Laser-induced desorption of NO from Si(111): effects of coverage on NO vibrational populations. Journal of Electron Spectroscopy and Related Phenomena, 1990, 54-55, 181-190.	0.8	17
121	High efficiency, dual collection mode near-field scanning optical microscope. Journal of Vacuum Science & Technology an Official Journal of the American Vacuum Society B, Microelectronics Processing and Phenomena, 1998, 16, 1948.	1.6	17
122	Imaging and autocorrelation of ultrafast infrared laser pulses in the 3–11-μm range with silicon CCD cameras and photodiodes. Optics Letters, 2001, 26, 238.	1.7	17
123	Interface characterization of molecular-monolayer/SiO2 based molecular junctions. Solid-State Electronics, 2006, 50, 1088-1096.	0.8	17
124	Attachment of a Diruthenium Compound to Au and SiO <sub>2</sub> /Si Surfaces by "Click―Chemistry. Langmuir, 2014, 30, 10280-10289.	1.6	17
125	Morphology of a thermally stable small molecule OPV blend comprising a liquid crystalline donor and fullerene acceptor. Journal of Materials Chemistry A, 2019, 7, 16458-16471.	5.2	17
126	Photodissociation dynamics of Mo(CO)6 at 266 and 355 nm: CO photofragment kineticâ€energy and internalâ€state distributions. Journal of Chemical Physics, 1991, 94, 7937-7950.	1.2	16

#	Article	IF	CITATIONS
127	Nonlinear optics as a detection scheme for biomimetic sensors: SFG spectroscopy of hybrid bilayer membrane formation. , 1999, , .		16
128	Reduced bimolecular recombination in blade-coated, high-efficiency, small-molecule solar cells. Journal of Materials Chemistry A, 2017, 5, 6893-6904.	5.2	16
129	Adsorption and photodecomposition of Mo(CO)6 on Si(111) 7×7: An infrared reflection absorption spectroscopy study. Journal of Chemical Physics, 1994, 100, 3187-3200.	1.2	15
130	Thin Film Elastic Modulus of Degradable Tyrosine-Derived Polycarbonate Biomaterials and Their Blends. Macromolecules, 2009, 42, 1212-1218.	2.2	15
131	Toward Fast Screening of Organic Solar Cell Blends. Advanced Science, 2020, 7, 2000960.	5.6	15
132	Near-field scanning optical microscopy incorporating Raman scattering for vibrational mode contrast. Surface Science, 1999, 433-435, 48-52.	0.8	14
133	In Situ Studies of the Swelling by an Electrolyte in Electrochemical Doping of Ethylene Glycol-Substituted Polythiophene. ACS Applied Materials & Interfaces, 2022, 14, 29052-29060.	4.0	13
134	Role of the electronically-active amorphous state in low-temperature processed In <sub>2</sub> O <sub>3</sub> thin-film transistors. Materials Advances, 2020, 1, 167-176.	2.6	12
135	Broadband Coherent Anti-Stokes Raman Spectroscopy Characterization of Polymer Thin Films. Applied Spectroscopy, 2006, 60, 1097-1102.	1.2	10
136	Characterization of SiGe Films for Use as a National Institute of Standards and Technology Microanalysis Reference Material (RM 8905). Microscopy and Microanalysis, 2010, 16, 1-12.	0.2	10
137	The Structural Origin of Electron Injection Enhancements with Fulleropyrrolidine Interlayers. Advanced Materials Interfaces, 2016, 3, 1500852.	1.9	10
138	Molecular Orientation Depth Profiles in Organic Glasses Using Polarized Resonant Soft X-ray Reflectivity. Chemistry of Materials, 2020, 32, 6295-6309.	3.2	10
139	The role of orientation in the MEL response of OLEDs. Journal of Materials Chemistry C, 2021, 9, 10052-10064.	2.7	10
140	Photodecomposition dynamics of Mo(CO)6/Si(111) 7×7: CO internal state and translational energy distributions. Journal of Chemical Physics, 1993, 98, 7651-7654.	1.2	9
141	Three Dimensionally Structured CdTe Thin-Film Photovoltaic Devices with Self-Aligned Back-Contacts: Electrodeposition on Interdigitated Electrodes. Journal of the Electrochemical Society, 2009, 156, H654.	1.3	9
142	Complex species and pressure dependence of intensity scaling laws for contamination rates of EUV optics determined by XPS and ellipsometry. Proceedings of SPIE, 2010, , .	0.8	9
143	Optics contamination studies in support of high-throughput EUV lithography tools. Proceedings of SPIE, 2011, , .	0.8	9
144	Proton NMR study of the orientation and motion of H2O in Na β′′ alumina. Journal of Chemical Physics, 1982, 76, 6-9.	1.2	8

#	Article	lF	CITATIONS
145	Influence of secondary tip shape on illumination-mode near-field scanning optical microscopy images. Journal of the Optical Society of America A: Optics and Image Science, and Vision, 1999, 16, 1936.	0.8	8
146	In situ measurement of annealing-induced line shape evolution in nanoimprinted polymers using scatterometry. Proceedings of SPIE, 2009, , .	0.8	8
147	Probing Crystallization Effects when Processing Bulk-Heterojunction Active Layers: Comparing Fullerene and Nonfullerene Acceptors. Chemistry of Materials, 2021, 33, 657-667.	3.2	8
148	A synchrotron beamline for extreme-ultraviolet photoresist testing. Review of Scientific Instruments, 2011, 82, 073102.	0.6	7
149	Coating Thickness Controls Crystallinity and Enables Homoepitaxial Growth of Ultraâ€Thinâ€Channel Bladeâ€Coated In <sub>2</sub> O <sub>3</sub> Transistors. Advanced Electronic Materials, 2020, 6, 2000354.	2.6	7
150	Cosolvent Effects When Blade-Coating a Low-Solubility Conjugated Polymer for Bulk Heterojunction Organic Photovoltaics. ACS Applied Materials & Interfaces, 2020, 12, 27416-27424.	4.0	7
151	Summary Abstract: The kinetics of CO dissociation on Fe(111). Journal of Vacuum Science and Technology A: Vacuum, Surfaces and Films, 1987, 5, 538-539.	0.9	6
152	Photodecomposition of Mo(CO)6/Si(111) 7×7: CO stateâ€resolved evidence for excited state relaxation and quenching. Journal of Chemical Physics, 1994, 101, 2929-2939.	1.2	6
153	Reply to: Triplet-triplet annihilation in rubrene/C60 OLEDs with electroluminescence turn-on breaking the thermodynamic limit. Nature Communications, 2019, 10, 4684.	5.8	6
154	Polarization Dependence of Charge Conduction in Conjugated Polymer Films Investigated with Time-Resolved Terahertz Spectroscopy. Journal of Physical Chemistry C, 2020, 124, 6993-7006.	1.5	6
155	Proton NMR of H 2 O in single crystal Li β and mixed β″ aluminas. Solid State Ionics, 1981, 5, 229-231.	1.3	5
156	The NIST EUV facility for advanced photoresist qualification using the witness-sample test. , 2011, , .		5
157	Surface plasmon polariton Raman microscopy. Vibrational Spectroscopy, 2012, 60, 85-91.	1.2	5
158	Charge transport and mobility relaxation in organic bulk heterojunction morphologies derived from electron tomography measurements. Journal of Materials Chemistry C, 2020, 8, 15339-15350.	2.7	5
159	Photodesorption dynamics of CO from Si (111): the role of surface defects. Surface Science, 1994, 321, 127-132.	0.8	4
160	Morphology Changes Upon Scaling a High-Efficiency, Solution-Processed Solar Cell From Spin-Coating to Roll-to-Roll Coating. Energy and Environmental Science, 2016, 9, .	15.6	4
161	Distinguishing between nonlinear channel transport and contact effects in organic FETs. Proceedings of SPIE, 2007, , .	0.8	3
162	SEIRAS Study of Chloride-Mediated Polyether Adsorption on Cu. Journal of Physical Chemistry C, 2018, 122, .	1.5	3

#	Article	IF	CITATIONS
163	Chemical imaging with scanning near-field infrared microscopy and spectroscopy. , 2000, , .		2
164	The hole in the bucky: structure-property mapping of closed- vs. open-cage fullerene solar-cell blends via temperature/composition phase diagrams. Journal of Materials Chemistry C, 0, , .	2.7	2
165	Long-Wavelength Instabilities Impact Alignment during Blade Coating of a Stretchable Organic Transistor Blend. ACS Applied Materials & Interfaces, 2022, 14, 1537-1545.	4.0	2
166	Assessment of sensitivity advances in near-field Raman spectroscopy. , 2000, , .		1
167	IR Spectroscopic Characterization of the Buried Metal Interface of Metal-Molecule-Silicon Vertical Diodes. AIP Conference Proceedings, 2005, , .	0.3	1
168	Structural and Morphological Characterization of Novel Organic Electrochemical Transistors via Four-dimensional (4D) Scanning Transmission Electron Microscopy. Microscopy and Microanalysis, 2021, 27, 1792-1794.	0.2	1
169	Thin film microstructure of solution processable pyrene-based small molecules for electronic applications. , 2007, , .		0
170	Nonlinear Vibrational Spectroscopy. Springer Series in Surface Sciences, 2013, , 137-161.	0.3	0
171	Anisotropic Charge Conduction in Oriented Donor-Acceptor Polymer Films and Liquid Dispersions Measured by Time-Resolved Terahertz Spectroscopy. , 2020, , .		0